Bioresource Technology 358 (2022) 127361

Contents lists available at ScienceDirect

Bioresource Technology

journal homepage: www.elsevier.com/locate/biortech

Biofilm disruption enhances growth rate and carbohydrate-active enzyme production in anaerobic fungi

Patrick A. Leggieri [a], Megan T. Valentine [b], Michelle A. O'Malley [a,c,*]

[a] Department of Chemical Engineering, University of California, Santa Barbara, CA 93106, USA
[b] Department of Mechanical Engineering, University of California, Santa Barbara, CA 93106, USA
[c] Joint BioEnergy Institute (JBEI), Emeryville, CA 94608, USA

HIGHLIGHTS

- Biofilm disruption increases growth and xylan degradation rates in *C. churrovis.*
- Biofilm disruption enhances catabolic CAZyme expression in *C. churrovis.*
- Metabolic fluxes and fermentation products are not altered by biofilm disruption.
- Rhizoidal *N. lanati* grows faster with stirring on a solid plant substrate.
- Stirred culture offers a path for scaled-up biomass valorization by anaerobic fungi.

ARTICLE INFO

Keywords:
Lignocellulose
Bioprocessing
Anaerobic fungi
Biofilms
Differential expression

ABSTRACT

Anaerobic gut fungi (AGF) are lignocellulose degraders that naturally form biofilms in the rumen of large herbivores and in standard culture techniques. While biofilm formation enhances biomass degradation and carbohydrate-active enzyme (CAZyme) production in some bacteria and aerobic fungi, gene expression and metabolism in AGF biofilms have not been compared to non-biofilm cultures. Here, using the tunable morphology of the non-rhizoidal AGF, *Caecomyces churrovis*, the impacts of biofilm formation on AGF gene expression, metabolic flux, growth rate, and xylan degradation rate are quantified to inform future industrial scale-up efforts. Contrary to previous findings, *C. churrovis* upregulated catabolic CAZymes in stirred culture relative to biofilm culture. Using a *de novo* transcriptome, 197 new transcripts with predicted CAZyme function were identified. Stirred cultures grew and degraded xylan significantly faster than biofilm-forming cultures with negligible differences in primary metabolic flux, offering a way to accelerate AGF biomass valorization without altering the fermentation product profile. The rhizoidal AGF, *Neocallimastix lanati*, also grew faster with stirring on a solid plant substrate, suggesting that the advantages of stirred *C. churrovis* cultures may apply broadly to other AGF.

1. Introduction

Anaerobic gut fungi (AGF) native to the rumen of large herbivores are potent lignocellulose degraders with potential for industrial valorization of crude biomass (Hooker et al., 2019). Their diverse repertoire of biomass-degrading carbohydrate-active enzymes (CAZymes) enables physical association with plant substrates to facilitate mass transfer of hydrolytic enzymes and metabolites (Lillington et al., 2020). Most characterized AGF are rhizoidal (Hanafy et al., 2020), such as *Neocallimastix lanati* pictured in Fig. 1**A**, and form dense biofilm-like mats as their rhizoids entangle with solid substrates and other microbial biomass.

Biofilm formation enhances the rate and extent of biomass degradation in many cellulolytic microbes (Brethauer et al., 2020) and has been linked to increased cellulase activity (Chahal, 1985; Gamarra et al., 2010; Xiros and Studer, 2017) and upregulation of CAZymes in

* Corresponding author.
E-mail addresses: leggieri@ucsb.edu (P.A. Leggieri), valentine@engineering.ucsb.edu (M.T. Valentine), momalley@ucsb.edu (M.A. O'Malley).

https://doi.org/10.1016/j.biortech.2022.127361
Received 3 April 2022; Received in revised form 7 May 2022; Accepted 19 May 2022
Available online 21 May 2022

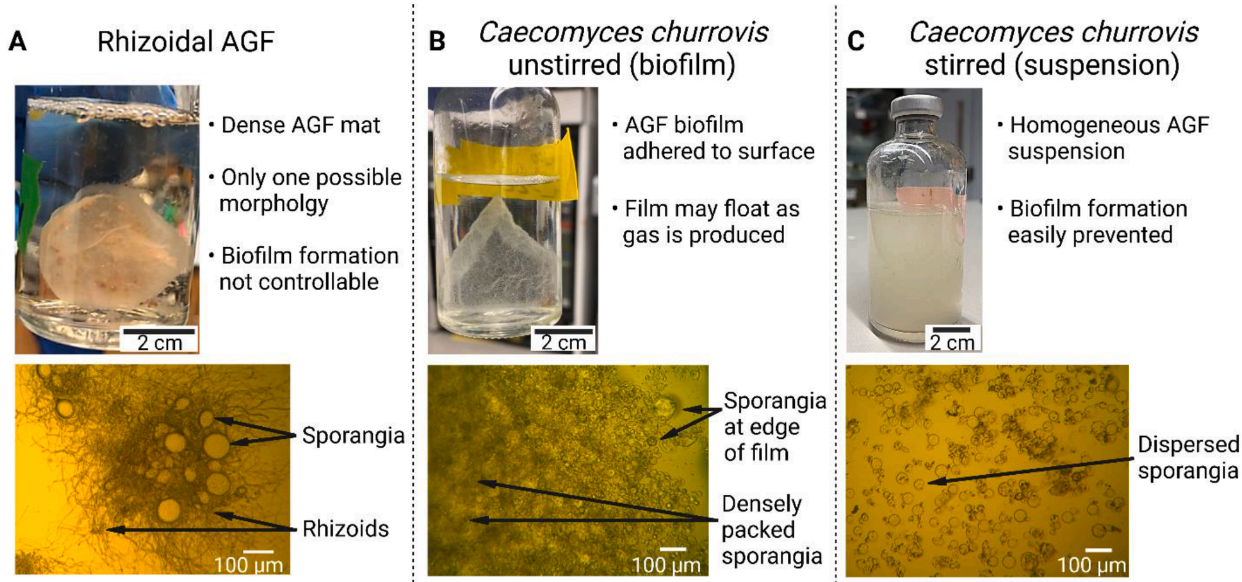

Fig. 1. **A)** Rhizoidal AGF, which comprise the majority of AGF sequenced to date, only grow in mats as the rhizoids of multiple sporangia entangle with each other. This cannot be avoided, therefore biofilm formation in rhizoidal AGF cannot be controlled. Pictured: *N. lanati*. **B)** The non-rhizoidal morphology of *C. churrovis* enables control of biofilm formation. *C. churrovis* forms biofilms adhered to the culture surface when cultured without stirring. When mounted on a slide, films appear thick and dense at the interior, with less tightly packed sporangia at the edge of the film. **C)** When continuously stirred, *C. churrovis* forms more homogeneous, nearly monodisperse cell suspensions, not biofilms.

anaerobic bacteria (Dumitrache et al., 2017) and aerobic fungi (Gamarra et al., 2010; Zhao et al., 2019) relative to planktonic[1] cultures. By contrast, the formation of biofilms by AGF cultures is not well described in the literature, and the biological advantage and function of biofilm formation in AGF remain unknown.

In particular, the effects of biofilm formation on AGF growth rates, substrate degradation rates, metabolic fluxes, and gene expression have not been studied. Gene expression and metabolism may vary substantially between biofilm and planktonic cultures of the same organism, therefore detailed understanding of the physiological effects of biofilm formation is required to design microbial systems for robust biomass conversion. This is especially important for industrial scale-up, as large-scale anaerobic cultures may benefit from agitation for accelerated mass transfer, which could disrupt naturally forming biofilm structures in both rhizoidal and non-rhizoidal AGF.

Typically, rhizoidal AGF grow exclusively in "mat" morphologies. The lack of well-mixed, suspension-based cultures precludes the use of non-biofilm control cultures and limits the ability to isolate the effects of biofilm formation using most standard AGF culture techniques. It is noted that rhizoidal AGF mats may not fit the technical definition of a bacterial-derived biofilm, as they are composed primarily of entangled extracellular rhizoids enriched in polysaccharides like chitin, rather than solely secreted extracellular polymeric substances (EPS) (Brethauer et al., 2020; Chandrasekar and Manavathu, 2008).

To allow for direct comparisons between biofilm-forming and suspended cultures, the focus here is on a non-rhizoidal AGF, *Caecomyces churrovis*. *C. churrovis* presents similar metabolism (97% of EC numbers shared with at least one other AGF) and CAZyme profiles to rhizoidal AGF (Brown et al., 2021; Henske et al., 2017; Leggieri et al., 2021). However, *C. churrovis* forms biofilms when cultured without stirring (Fig. 1**B**), and forms nearly monodisperse cell suspensions in stirred culture (Fig. 1**C**). Thus, *C. churrovis* allows for quantitative analysis of the direct effects of biofilm formation on AGF growth, gene expression, and metabolic flux. It is argued herein that understanding the effects of biofilm disruption and shear on gene expression and flux in *C. churrovis* can inform the understanding of the mechanisms and consequences of biofilm formation, as well as industrial scale-up efforts for all AGF (Gruninger et al., 2014; Vinzelj et al., 2020), even though the phenotypic response to shear may differ in rhizoidal strains.

Here, a simple pipeline to isolate the impact of biofilm formation on AGF growth and functional properties using *C. churrovis* as a model system is presented. Via differential gene expression analysis in unstirred biofilm-forming cultures vs. stirred cultures of suspended planktonic cells, the effects of biofilm formation on the expression of biomass-degrading CAZymes, primary metabolic enzymes, substrate binding proteins, and other gene types are quantified. Obtained RNA-Seq transcriptional data are aligned to the existing *C. churrovis* genome, and a *de novo* transcriptome of the unmapped transcripts is assembled to uncover previously unannotated CAZymes and search for proteins potentially involved in biofilm formation. Growth rates, xylan degradation rates, and metabolic fluxes are measured in the stirred and biofilm cultures. Interestingly, while growth and xylan degradation were significantly faster in stirred cultures, few primary metabolic enzymes were differentially expressed, and accordingly, primary metabolic fluxes were not significantly altered. A significant number of differentially expressed genes and *de novo* transcripts could not be annotated, although some showed homology to proteins in other biofilm-forming organisms. Several of the unannotatable genes and *de novo* transcripts clustered by sequence similarity, potentially laying a foundation for the discovery of the genes responsible for AGF biofilm formation. Further, the rhizoidal AGF, *Neocallimastix lanati*, showed significantly faster growth and biogas production on a solid plant biomass substrate in stirred culture than in unstirred culture, suggesting that the results observed in *C. churrovis* may potentially apply to other AGF and motivating the design of agitated/continuous AGF culture systems for CAZyme production and biomass conversion.

[1] In some of these studies, "submerged" culture denotes non-biofilm cultures, as the biofilms are either grown on plates or membrane reactors. In this study, stirred and unstirred cultures are both submerged in liquid medium, but only unstirred cultures form biofilms.

2. Materials and methods

2.1. Culture of anaerobic gut fungi

A fully defined, modified version of anaerobic Medium B (MB) (Leggieri et al., 2021; Theodorou et al., 1995) was used for both routine culture and growth experiments. The headspace of AGF cultures was 5% H_2, 35% CO_2, balance N_2. All cultures were grown at 39 °C in 75 mL anaerobic serum bottles with 45 mL of liquid medium. AGF were grown on xylan (from corn core, TCI America, Portland, OR) or dried, milled reed canary grass (milled with a 4 mm screen size, provided by the US Department of Agriculture, Agricultural Research Service, US Dairy Forage Research Center) at final concentrations of 5 g/L and 10 g/L, respectively.

Caecomyces churrovis was previously isolated from the feces of a large herbivore (Henske et al., 2017), and *Neocallimastix lanati* was isolated from the feces of a sheep (Wilken et al., 2021). For routine culture, AGF were transferred to new media every 2 days. In all growth experiments, starter cultures of AGF were grown for 48 h and used for inoculation. All inoculums were 10% v/v. Growth of AGF was monitored using the pressure accumulation method described previously (Henske et al., 2018a; Henske et al., 2018b), which aligns with *C. churrovis* concentrations measured *via* optical density and dry cell weight (Leggieri et al., 2021) and *N. lanati* dry cell weight concentrations (Wilken et al., 2021).

Stirred cultures were grown with one 25 mm cylindrical magnetic stir bar in each bottle (autoclaved in the bottle) (Part No. SWN660, Globe Scientific, Mahwah, NJ) with constant stirring at 100 rpm on a VELP 15-position digital magnetic stir plate (Part No. F203A0180, VELP Scientifica, Usmate Velate, MB, Italy). Unstirred biofilm cultures were grown identically to stirred cultures, except with no stir bars in the bottles.

Alongside three blank media bottles, six biological replicate *C. churrovis* cultures were grown for each condition. Three were harvested for RNA extraction, and three were used to complete the growth and metabolite curves. *N. lanati* was also grown using three biological replicate cultures for each condition alongside three blank media bottles.

2.2. Microscopy

AGF were imaged using a Zeiss Primovert transmitted light microscope (Part No. 415510–1101-000, Carl Zeiss Microscopy GmbH, Göttingen, Germany). Samples were imaged with a 10× air objective using a slide and coverslip without fixation. Images were collected and analyzed using a SPOT Idea 28.2 5-MP camera and the SPOT 5.1 imaging software (SPOT Imaging, Sterling Heights, MI). Lateral magnification was 2.5 μm/pixel.

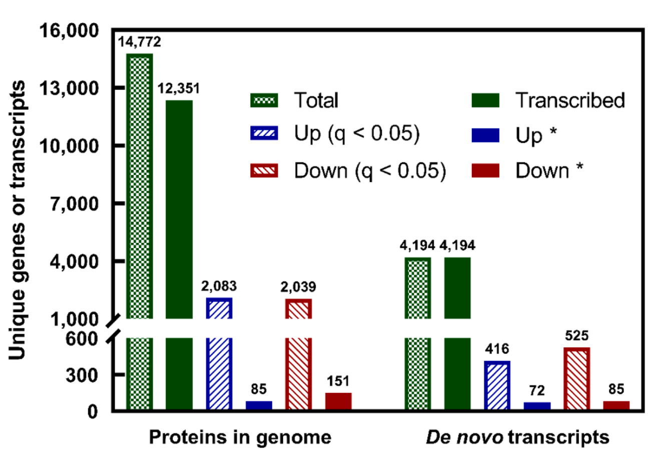

Fig. 2. Total proteins in the *C. churrovis* genome, *de novo* transcripts assembled, and statistically significant up- and down-regulated genes (in biofilms) shown in dashed bars (using only $q < 0.05$). Transcribed, and significantly differentially expressed with cutoffs (marked with *, $q < 0.05$, $\log_2$fold change > 1.5, max TPM > 2) genes shown in solid bars.

2.3. High performance liquid chromatography (HPLC) and gas chromatography (GC) analysis of metabolites

HPLC analysis was conducted as described previously (Leggieri et al., 2021). Xylan and ethanol were detected using a refractive index detector; succinate, lactate, formate, fumarate, and acetate were detected using a variable wavelength detector set to 210 nm. Standards were created for all sugars and metabolites in deionized water at 1%, 0.1%, and 0.01% w/v concentrations and the above protocol was followed to run each standard. Standard curves were created via linear regression; R^2 values ranged from 0.9996 to 1.000.

Hydrogen was quantified *via* GC as described previously (Leggieri et al., 2021). Hydrogen standards including 500 ppm H_2, 2% H_2, 5% H_2, and 20% H_2 with balance helium (Douglas Fluid & Integration Technology, Prosperity, SC), were run at each measurement timepoint to account for the detector baseline that varied slightly each day. Standard curves were created via linear regression; R^2 values ranged from 0.9890 to 0.9979.

Metabolic flux measurements for each metabolite were calculated based on measurements one and two days after inoculation as follows: the difference in amount (mmol) of that metabolite in each culture divided by the average calculated AGF mass (gram dry weight, GDW) present in the culture bottle during that time, divided by the elapsed time between the two measurements. Flux units reported here are mmol $GDW^{-1}h^{-1}$.

2.4. RNA extraction, library preparation, and sequencing

The volume of each culture to harvest for RNA extraction was calculated to yield approximately the same mass of AGF cells. At the time of harvesting, a sample from each culture was added to RNAlater (Part No. R0901, Sigma-Aldrich, St. Louis, MO) in a 1:1 volume ratio and immediately centrifuged for 20 minutes at 4 °C and 12,000g. Following centrifugation, supernatants were removed, and each sample was flash-frozen in liquid nitrogen and stored at -80 °C for one week.

Cell pellet samples were removed from storage, thawed on ice, and lysed via liquid nitrogen grind using a pestle and mortar. Total RNA was then extracted from each lysed cell pellet with the RNeasy Mini Kit (Qiagen, Hilden, Germany) following the provided protocol for filamentous fungi, including the QIAshredder (Part No. 79656, Qiagen) and on-column DNAse digest (Part No. 79254, Qiagen). 3 μL aliquots were taken from each purified RNA sample for quantification and quality analysis with a Qubit (Part No. Q33327, Thermo-Fisher Scientific) and TapeStation (Agilent), respectively. All RNA samples had RINe values above 9 and concentrations above 100 ng/μL.

Stranded RNA-Seq libraries were created with the NEBNext Ultra II RNA Library Prep Kit for Illumina (Part No. E7775, New England BioLabs, Ipswich, MA) and quantified via qPCR. Libraries were sequenced in the Biological Nanostructures Lab at the University of California, Santa Barbara using an Illumina NextSeq 500 with high output and 75 basepair single end reads (Illumina, San Diego, CA).

2.5. RNA-Seq data analysis

Filtered reads from each library were checked for quality using fastQC [https://www.bioinformatics.babraham.ac.uk/projects/fastqc/] and trimmed with Trimmomatic (Bolger et al., 2014). The *C. churrovis* genome was downloaded from Mycocosm [https://mycocosm.jgi.doe.gov/] and proteins with duplicate sequences within the genome were removed except for one representative protein (with the lowest protein ID). Trimmed reads were then aligned to this duplicate-checked *C. churrovis* genome using HISAT2 (Kim et al., 2019). StringTie2

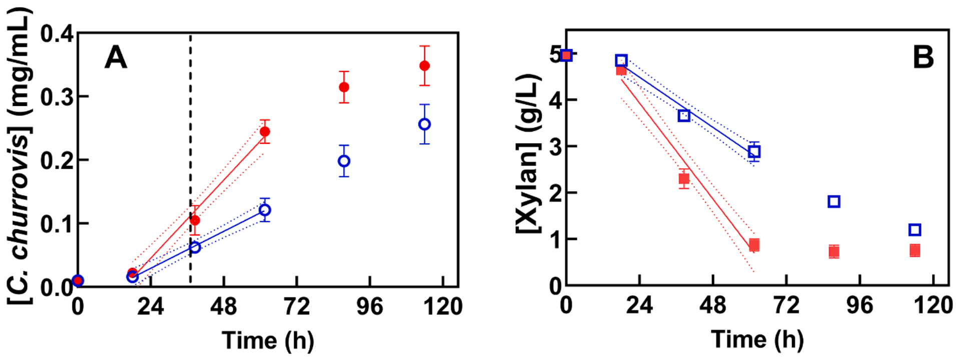

Fig. 3. A) *C. churrovis* grew significantly faster on xylan when stirred (solid red points) compared to unstirred (hollow blue points), $p < 0.0001$. Dashed line represents time of harvest for RNA extraction during mid-exponential growth. **B)** *C. churrovis* degraded xylan significantly faster in stirred culture (solid red points) than in unstirred culture (hollow blue points), $p < 0.0001$. Dotted lines represent the 95% confidence intervals of each regression. (For interpretation of the references to colour in this figure legend, the reader is referred to the web version of this article.)

(Kovaka et al., 2019) was used to assemble splice-aware transcripts from the aligned reads and to assemble *de novo* transcripts from the unaligned reads (6.1% of the total reads). *De novo* transcripts that overlapped with existing genes in the genome were removed; the reads initially attributed to those *de novo* transcripts were assigned to the existing genes with which they overlapped. DESeq2 (Love et al., 2014) was used to determine which genes showed statistically significant per-cell differential expression between the stirred and unstirred culture conditions.

To provide greater statistical specificity for phenotypic changes in stirred vs. biofilm cultures, stringent requirements beyond $q < 0.05$ were imposed for a gene to be considered significantly differentially expressed. Namely, each protein or *de novo* transcript must also have a $\log_2$fold change > 1.5 (magnitude) between conditions to select for large-magnitude differences in expression, and TPM > 2 to omit genes that are extremely low in transcript number but technically meet the $q < 0.05$ cutoff. While no universally accepted TPM cutoff threshold exists for differential expression analysis, one is included here to omit extremely low-abundance transcripts (or sequencing/assembly artifacts) from the differentially expressed gene sets (*e.g.,* 10 total transcript reads in stirred cultures and 0 in unstirred cultures). Fig. 2 shows the number of detected transcripts that mapped to the genome or were assembled as *de novo* transcripts, the number of these genes/transcripts that were differentially expressed ($q < 0.05$), and significantly differentially expressed according to the more stringent cutoffs. As seen in Fig. 2, these cutoffs substantially reduce the number of genes/transcripts that are considered significantly differentially expressed.

CloudBLAST (Matsunaga et al., 2008) was used to annotate *de novo* transcripts assembled by StringTie2. Conserved protein domains within unannotated genes and *de novo* transcripts were identified using the Conserved Domain Search (CD-Search) tool (Lu et al., 2020; Marchler-Bauer and Bryant, 2004). CAZyme annotations were assigned to genes and *de novo* transcripts based on functional annotations in Mycocosm (Grigoriev et al., 2014) and dbCAN (Yin et al., 2012), using a cutoff of two tools to determine CAZyme classification. Gene Ontology (GO) numbers (The Gene Ontology Consortium, 2021; The Gene Ontology Consortium et al., 2000) and CAZyme annotations were assigned to detected genes and *de novo* transcripts using Python. DeepLoc (Almagro Armenteros et al., 2017) was used to localize transcripts to the cytosol, hydrogenosome, or other cellular compartments; here, it is assumed that localization to the mitochondria or plastid corresponds to the hydrogenosome in AGF. SignalP 5.0 was used to determine which genes are most likely secreted (Almagro Armenteros et al., 2019). UCLUST (Edgar, 2010) was used to cluster unannotated *de novo* transcripts and "hypothetical proteins" that aligned to the *C. churrovis* genome based on sequence similarity.

2.6. Statistical analysis

All statistical analyses (other than determination of differential expression with DESeq2) were conducted using the Prism 9.1.2 software (GraphPad, San Diego, CA). Prism 9.1.2 was used to (*i*) interpolate the concentrations of metabolites detected via HPLC and GC using standard curves, (*ii*) determine significant differences in growth rates and metabolite fluxes between growth conditions via *t*-tests, (*iii*) and conduct contingency tests (Fisher's Exact Tests) to determine significant up/downregulation of gene classes (a "class" being a particular CAZyme type, a GO term, etc.). Although most gene classes showed some genes significantly upregulated and some genes significantly downregulated in biofilm culture, Fisher's Exact Test determines whether a gene class is significantly overrepresented in the up/downregulated gene sets based on the number of genes in that class within the genome or transcriptome, the total number of genes in the genome or transcriptome, and the total number of genes up/downregulated. In all statistical tests, $\alpha = 0.05$ was used.

Table 1
Differentially expressed CAZymes labeled by CAZyme type. Fisher's Exact Tests show that the catabolic CAZyme classes (glycoside hydrolase, pectin lyase, carbohydrate esterase) are significantly downregulated in biofilm culture relative to stirred culture ($p < 0.05$). No CAZyme classes are significantly upregulated in biofilm culture relative to stirred culture. 197 *de novo* CAZyme transcripts that did not map to the existing *C. churrovis* genome were identified, along with 47 transcripts with DOC2 domains (see supplementary material).

CAZyme type	CAZyme count in genome	CAZyme count in *de novo* transcriptome	Genes upregulated	Genes downregulated	p-value Up	p-value Down
Glycoside hydrolase	304	81	5	15	0.2544	**0.0001**
Pectin lyase	9	11	1	3	0.1532	**0.0019**
Carbohydrate esterase	257	23	1	8	0.7329	**0.0243**
Glycosyltransferase	137	12	0	0	0.6385	0.2692
Carbohydrate binding module	504	70	5	11	0.8139	0.1747
Dockerin domains (DOC2)	392	47	6	9	0.1842	0.1243

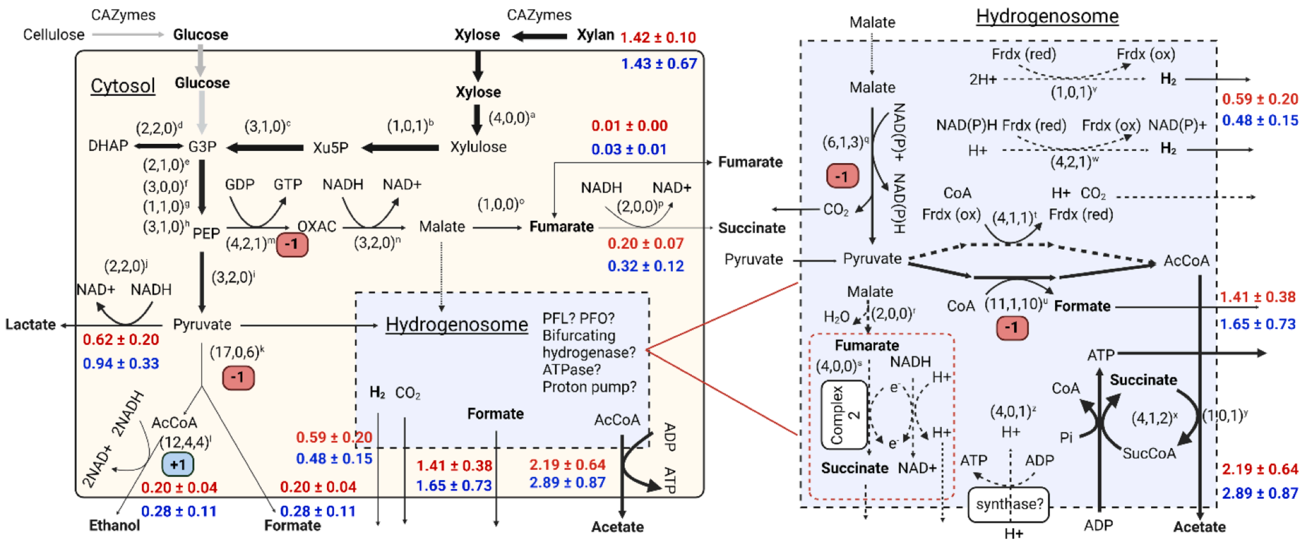

Fig. 4. Fluxes and expression of central metabolism (glycolysis, hydrogenosome, TCA cycle) of stirred and unstirred *C. churrovis* cultures. Fluxes in red represent stirred cultures, blue represent unstirred cultures. No fluxes differed significantly. Expression statistics are reported for each enzyme as (number of unique transcripts detected, number of upregulated transcripts, number of downregulated transcripts) using q < 0.05 as the only threshold for significance. Enzymes meeting the $\log_2$fold-change and TPM thresholds are denoted with numbers in colored boxes (blue: significantly upregulated in biofilms, red: significantly downregulated). Enzymes [with EC numbers if available]: **a)** xylose isomerase [5.3.1.5] **b)** xylulokinase [2.7.1.17] **c)** glycoaldehydetransferase [2.2.1.1] **d)** triose-phosphate isomerase [5.3.1.1] **e)** glyceraldehyde 3-phosphate (G3P) dehydrogenase [1.2.1.12] **f)** phosophoglycerate kinase [2.7.2.3] **g)** G3P dehydrogenase (NADP+) [1.2.1.9] **h)** phosphopyruvate hydratase [4.2.1.11] **i)** PEP synthase [2.7.9.2] **j)** lactate dehydrogenase [1.1.1.28] **k)** pyruvate formate-lyase (PFL) cytosolic [2.3.1.54] **l)** alcohol dehydrogenase [1.1.1.1] **m)** PEP carboxykinase [4.1.1.32] **n)** malate dehydrogenase [1.1.1.37] **o)** fumarase cytosolic [4.2.1.2] **p)** succinate dehydrogenase [1.3.5.1] **q)** malic enzyme [1.1.1.40] **r)** fumarase hydrogenosomal [4.2.1.2] **s)** complex 2 subunits A, B, C, D **t)** pyruvate ferredoxin oxidoreductase (PFO) **u)** PFL hydrogenosomal [2.3.1.54] **v)** iron hydrogenase **w)** bifurcating hydrogenase subunits A, B, G **x)** succinyl coenzyme A (CoA) synthase **y)** acetate succinyl CoA transferase **z)** ATP synthase subunits A, B, G, D. Created with BioRender.com. (For interpretation of the references to colour in this figure legend, the reader is referred to the web version of this article.)

3. Results and discussion

3.1. Stirring prevents C. churrovis biofilm formation while enhancing xylan degradation and AGF growth

Stirring produces physical forces within microbial cultures that are expected to impact culture function. Stirring within AGF culture vessels introduces mixing and turbulence, thereby enhancing the mass transfer of substrates, enzymes, and metabolites to/from AGF cell surfaces, which is in turn expected to increase growth rates in AGF cultures which may be otherwise limited by diffusion. However, stirring also introduces shear stresses, which in *C. churrovis* disrupts biofilm formation. At present time, it is not understood if biofilm disruption by stirring impacts AGF phenotypes and culture outcomes.

To investigate the effects of stirring, the growth rate and xylan degradation rate of *C. churrovis* (Fig. 3**A and 3B**, respectively) were measured in stirred cultures and biofilm-forming cultures; both rates were significantly greater in stirred cultures ($p < 0.0001$, $p < 0.0001$ respectively). This suggests that growth of *C. churrovis* on xylan in biofilms is limited by diffusion, rather than its intrinsic growth rate. Further, the disruption of *C. churrovis* biofilms either does not elicit a phenotypic response that slows growth and xylan degradation, or these effects are outweighed by the mass transfer advantages of mixing. Therefore, biofilm disruption and culture mixing via stirring yields an easily achieved, potentially scalable *C. churrovis* phenotype for polysaccharide degradation.

3.2. Catabolic CAZymes are significantly upregulated in stirred, faster-growing C. churrovis cultures relative to biofilm-forming cultures

AGF are promising candidates for bioprocessing primarily thanks to their abundant and diverse repertoire of CAZymes. However, no prior studies have compared CAZyme expression in biofilm vs. non-biofilm AGF cultures, and bacterial and aerobic fungal literature suggests significant differences likely exist (Dumitrache et al., 2017; Gutiérrez-Correa et al., 2012; Zhao et al., 2019). As shown in Table 1, per-cell expression of the catabolic CAZyme classes (glycoside hydrolase, pectin lyase, carbohydrate esterase) was significantly upregulated in stirred cultures relative to biofilm-forming AGF cultures, as determined by Fisher's Exact Test (see supplementary material for a list of CAZymes identified in the *de novo* transcriptome with sequences).

While downregulation of catabolic CAZymes in AGF biofilms contrasts previous findings in cellulolytic bacteria and aerobic fungi (Dumitrache et al., 2017; Gutiérrez-Correa et al., 2012; Zhao et al., 2019), this may be due to slower, diffusion limited growth of the fungus in biofilms, rather than specific repression of CAZymes brought on by the biofilm morphology alone. It is likely that growth is enhanced in the well-mixed stirred cultures mostly due to enhanced mass transfer of enzymes and substrates, and that upregulation of catabolic CAZymes plays only a minor role in increasing growth rate.

In fact, the observed per-cell upregulation of catabolic CAZymes may be a consequence of faster growth in *C. churrovis*, rather than a cause. AGF downregulate CAZymes in response to increased concentration of monosaccharides released from polysaccharides (Henske et al., 2018a; Henske et al., 2018b; Solomon et al., 2016). They may also downregulate CAZymes under increased concentration of growth-inhibiting metabolic end products like formate and acetate. In co-culture with a methanogen, a system shown to grow faster than AGF mono-culture likely due to methanogen uptake of formate and hydrogen (Leggieri et al., 2021), *C. churrovis* upregulated some CAZymes relative to mono-culture (Swift et al., 2019). In turbulent stirred cultures, these inhibitors and monosaccharides (secreted or produced at or near the cell surface) are in lower local concentration near the cells than in biofilm cultures in which they diffuse away from the cells on timescales that could influence gene expression (Shamir et al., 2016).

Taken together, the results presented here and previous findings

Table 2
Enrichment analysis of significantly down-regulated and up-regulated GO IDs determined by Fisher's Exact Test. Several GO IDs enriched in the down-regulated gene set (more expressed with stirring) relate to cell wall catabolism (**bolded**). GO IDs enriched in the up-regulated gene set (more expressed in biofilms) appear unrelated.

GO ID	GO Name	GO Type	p-value
(A) Down-regulated (i.e., more expressed with stirring)			
GO:0004623	**phospholipase A2 activity**	Molecular function	0.0026
GO:0016042	**lipid catabolic process**	Biological process	0.0026
GO:0055085	transmembrane transport	Biological process	0.03055
GO:0009332	glutamate-tRNA ligase complex	Cellular component	0.03274
GO:0004818	glutamate-tRNA ligase activity	Molecular function	0.03601
GO:0009253	**peptidoglycan catabolic process**	Biological process	0.0376
GO:0016998	**cell wall catabolic process**	Biological process	0.03822
GO:0031681	G-protein beta-subunit binding	Molecular function	0.04001
GO:0008422	**beta-glucosidase activity**	Molecular function	0.04494
GO:0000750	pheromone-dependent signal transduction involved in conjugation with cellular fusion	Biological process	0.04501
GO:0003796	lysozyme activity	Molecular function	0.04778
(B) Up-regulated (i.e., more expressed in biofilms)			
GO:0008519	ammonium transmembrane transporter activity	Molecular function	0.009
GO:0004252	serine-type endopeptidase activity	Molecular function	0.0063
GO:0000796	condensin complex	Cellular component	0.0276
GO:0006508	proteolysis	Biological process	0.03279
GO:0070534	protein K63-linked ubiquitination	Biological process	0.03312
GO:0000974	Prp19 complex	Cellular component	0.0365
GO:0090730	Las1 complex	Cellular component	0.04106
GO:0001584	rhodopsin-like receptor activity	Molecular function	0.0414

show that in two distinct systems (stirred cultures and co-cultures with methanogens), upregulation of CAZymes in *C. churrovis* is correlated with faster fungal growth and decreased local concentration of metabolic inhibitors. While enhanced CAZyme production may be more of a consequence than a cause of faster AGF growth in turbulent culture, stirring is a simple approach to grow AGF more quickly and with more CAZymes produced per cell, offering an approach to scale up non-rhizoidal AGF cultures that may be uniformly sampled to assess and optimize culture conditions.

3.3. Metabolic fluxes and expression of primary metabolic enzymes are unchanged in stirred and biofilm-forming C. churrovis cultures

Primary metabolic flux determines the profile of fermentation products that can be made or used downstream for bioproduction. Therefore, it is critical to understand how biofilm disruption impacts AGF metabolic flux if stirring or agitation is to be used to control AGF growth. As shown in Fig. 4, no primary metabolic fluxes differed significantly between the stirred and unstirred cultures. Similarly, few primary metabolic enzymes were differentially expressed between the two conditions. While stirred cultures degraded xylan significantly faster, xylan flux did not differ between stirred and unstirred cultures, suggesting similar growth yields in both conditions (gDW/mol$_{xylan}$).

Many genes involved in primary metabolism showed q-values < 0.05, but with the TPM and log$_2$fold change cutoffs applied, only five primary metabolic enzymes were significantly differentially expressed. Pyruvate formate lyase (PFL) expression was upregulated in both the cytosol (k) and hydrogenosome (u) in stirred cultures. Increased PFL expression could also be a consequence of faster AGF growth rather than a direct cause, as its upregulation here did not lead to increased PFL flux. Like some CAZymes, PFL was upregulated in faster growing (Leggieri et al., 2021) co-cultures of *C. churrovis* with a methanogen (Brown et al., 2021), although PFL flux also increased in co-culture systems.

Other significantly differentially regulated genes include an alcohol dehydrogenase (l), which was upregulated in unstirred biofilm cultures, and a phosphoenolpyruvate decarboxylase (m) and malic enzyme (q), which were upregulated in stirred cultures. It is possible that the upregulation (in biofilms) of an ethanol-producing enzyme in a strictly cytosolic pathway and downregulation of two genes involved in malate production and eventual utilization in the hydrogenosome suggest a correlation between hydrogenosome activity and faster AGF growth (as shown in (Leggieri et al., 2021)). However, no significant differences in hydrogenosomal fluxes were observed, and the uncertainty of the hydrogenosomal pathways in Fig. 4 precludes quantitative assessment of this hypothesis.

The GO Enrichment analysis in Table 2 corroborates the phenotypic shift towards more plant cell wall catabolism in stirred cultures vs. biofilm cultures with negligible changes in primary metabolism. GO terms vary widely in specificity, however GO Enrichment analysis is useful to identify large-scale phenotypic differences between conditions if multiple related GO functions are overexpressed in one condition and not the other. The bold GO terms in Table 2**A** all relate to cell wall catabolism and/or hydrolysis of lignocellulose in plant cell walls, and they are all significantly overrepresented in the downregulated gene set and not the upregulated gene set, supporting the observed significant downregulation of the catabolic CAZyme classes in biofilm culture relative to stirred culture. In Table 2**B,** the overrepresented GO terms in biofilm cultures are not obviously connected to each other in a way that represents a phenotypic shift. This is expected, as AGF biofilm-forming machinery is unannotated and therefore lacks GO identification.

The combined gene expression and flux data suggest that primary metabolism is not significantly altered in AGF stirred vs. biofilm cultures. Interestingly, this implies that CAZyme expression and primary metabolic flux may not be correlated in AGF mono-cultures. Therefore, researchers may choose to stir AGF cultures for faster polysaccharide degradation and CAZyme production without altering the fermentation product profile.

3.4. Differential expression identifies proteins that may be associated with biofilm formation

AGF biofilm-forming genes, or other genes directly involved in response to shear or biofilm disruption, have not yet been identified and annotated. However, they would likely be secreted and upregulated in biofilm-forming vs. stirred AGF cultures. To search for these genes and spur future mechanistic research, the functions of the significantly differentially expressed unannotated genes and *de novo* transcripts, which comprise most of the dataset, were investigated. It is possible that biofilm-forming machinery is expressed in stirred cultures even though shear prevents biofilm development. Thus, unannotated genes and *de novo* transcripts downregulated in biofilm cultures were included in this search as well.

To annotate the significantly differentially expressed unannotated genes and *de novo* transcripts or identify homology with genes in known biofilm-forming organisms, the *de novo* transcripts and existing genes with "hypothetical protein" or "expressed protein" annotation were BLASTed via CloudBLAST (e-value threshold 10^{-4}, % ID > 70%). This resulted in putative annotation of 100 of the 236 significantly downregulated genes and *de novo* transcripts (42%) and 69 of the 157 significantly upregulated genes and *de novo* transcripts (44%). This BLAST did not reveal any obvious biofilm-related functionality; however, some of these differentially expressed genes with secretion tags could possibly be involved in extracellular biofilm formation or modification. Therefore, all significantly differentially expressed *de novo* transcripts and secreted proteins were BLASTed using more lenient parameters (e-value threshold 10^{-3}, % ID > 40%), identifying several proteins and *de novo* transcripts with homology to known biofilm and/or adhesion-related proteins, and even more proteins with no homology to any other proteins (see supplementary material).

The unannotated, significantly differentially expressed *de novo* transcripts and secreted proteins are candidates for further investigation into their role in AGF biofilm function. Many show homology to subtilisin-like proteins, extracellular serine proteases produced by the most widely studied model biofilm-forming bacterium, *Bacillus subtilis*. While subtilisins typically degrade extracellular biofilms (Leroy et al., 2008; Liu et al., 2021; Mitrofanova et al., 2017) rather than form them, their differential expression here suggests possible involvement in AGF biofilm growth and/or remodeling. As expected, more subtilisin-like secreted proteins and *de novo* transcripts were upregulated in biofilm cultures than downregulated. Protein 625875 could be influential to the mechanical properties of *C. churrovis* biofilms, as it is homologous with several eukaryotic titin-like proteins, large proteins which influence the elasticity of muscle tissues (Granzier and Labeit, 2004). Several differentially expressed *de novo* transcripts have chitin-binding GO annotations. While this GO category was not significantly overrepresented in the biofilm-upregulated gene set, these previously unannotated transcripts may participate in binding of AGF cell walls (predominantly made of chitin) to other cells and/or to substrates.

Some *C. churrovis* differentially expressed secreted “hypothetical proteins” and *de novo* transcripts showed no homology to any AGF proteins and could therefore contribute to *C. churrovis*’ unique morphology relative to the rest of the phylum (see supplementary material). Of these proteins present uniquely in *C. churrovis* (and no other AGF), some showed similarity with proteins involved extracellular cell adhesion or proteolysis, processes involved in biofilm formation and maturation. Others showed no appreciable homology to any known proteins and warrant further investigation to develop a better mechanistic understanding of whether or how they contribute to AGF biofilms.

Even after relaxing BLAST parameters, most significantly differentially expressed genes and *de novo* transcripts remained unannotated. To search these still-unannotated genes and transcripts for classes of proteins co-expressed to form biofilms or respond to shear, they were investigated for sequence similarity clustering. A greater proportion of the differentially expressed unannotated *de novo* transcripts clustered together (>25% sequence similarity) than the unannotated differentially expressed proteins in the *C. churrovis* genome (see supplementary material). These clusters of *de novo* transcripts were generally larger but showed lower sequence identity than the clusters of unannotated proteins in the genome.

While these clusters may be performing coordinated biological functions, their conserved protein domains showed no obvious relationships within each cluster, complicating discovery of co-regulated biofilm-implicated genes. However, their co-expression is at least correlated with either biofilm formation or stirred cultivation under shear. Therefore, their structures may be of interest for future investigation of AGF biofilm-forming or shear response machinery. A master spreadsheet of all detected genes and *de novo* transcripts, their expression statistics, their amino acid or nucleotide sequence, whether they are most likely secreted, and their functional annotation (with any CAZyme prediction) is provided for further investigation (see supplementary material).

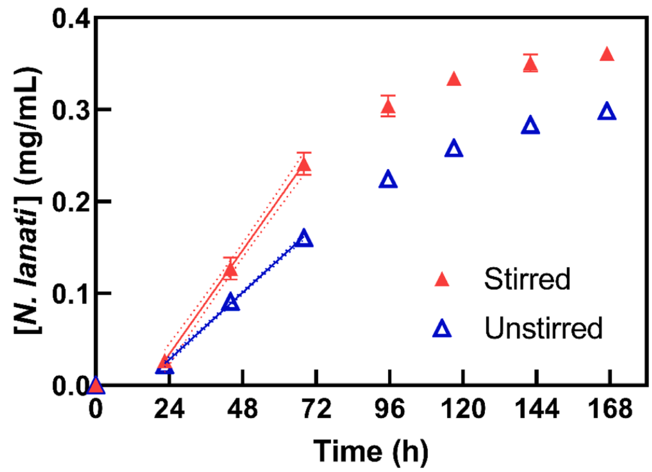

Fig. 5. Rhizoidal *N. lanati* grew significantly faster in stirred culture on a solid milled plant substrate compared to unstirred culture ($p < 0.0001$). Dotted lines represent the 95% confidence intervals of each regression.

3.5. Rhizoidal N. lanati grew significantly faster on solid milled grass with stirring

As shown, non-rhizoidal AGF such as *C. churrovis* have promise for industrial scale up; however, rhizoidal AGF comprise most of the phylum, and should therefore be considered for scale-up as well. To determine whether the growth advantages observed in *C. churrovis* on soluble substrates also occur in suspended cultures of rhizoidal AGF, the properties of stirred cultures of rhizoidal *N. lanati* on a milled grass substrate were tested.

Fig. 5 shows that stirred cultures of rhizoidal *N. lanati* on solid reed canary grass grew significantly faster than unstirred cultures ($p < 0.0001$). *N. lanati* growth requires physical association with the plant substrate, i.e., formation of small biofilms around the grass. Therefore, biofilm vs. non-biofilm direct comparison experiments are not achievable with this strain. However, these results suggest that physical association occurs in the turbulent stirred cultures, and the enhanced mass transfer introduced by stirring helps to accelerate AGF growth and biomass degradation. This is promising for use of rhizoidal AGF in mixed solid and liquid state cultures for future applications.

4. Conclusions

AGF, promising lignocellulose degraders, form biofilm-like mats which putatively facilitate biomass breakdown but have precluded industrial-scale cultures. In non-rhizoidal *C. churrovis*, biofilms are easily disrupted with stirring, thereby increasing AGF growth rate, catabolic CAZyme expression, and xylan degradation rate, with similar metabolic fluxes to biofilm-forming cultures. Stirring also increases the growth rate of rhizoidal *N. lanati* on solid plant substrate, a system that could resemble prototypical scaled-up AGF anaerobic digestion. Biofilm disruption in non-rhizoidal AGF *via* stirring enhances CAZyme production and polysaccharide degradation without altering the fermentation product profile, offering another knob to turn to optimize scaled, biomass-valorizing AGF cultures.

Data availability

Raw RNA-Seq reads are available at the BioProject ID: PRJNA816473. E-supplementary data for this work can be found in the e-version of this paper online.

CRediT authorship contribution statement

Patrick A. Leggieri: Conceptualization, Methodology, Investigation, Writing – original draft, Writing – review & editing. **Megan T. Valentine:** Conceptualization, Supervision, Funding acquisition, Writing – review & editing. **Michelle A. O'Malley:** Conceptualization, Supervision, Funding acquisition, Writing – review & editing.

Declaration of Competing Interest

The authors declare that they have no known competing financial interests or personal relationships that could have appeared to influence the work reported in this paper.

Acknowledgements

The authors acknowledge funding support from the Army Research Office via contract W911NF-19-1-0010, the California NanoSystems Institute (CNSI) Challenge Grant Program, and the U.S. Department of Energy (DOE) (DE-SC0020420). The authors further thank Dr. Jennifer Smith for library preparation and sequencing.

Appendix A. Supplementary data

Supplementary data to this article can be found online at https://doi.org/10.1016/j.biortech.2022.127361.

References

Almagro Armenteros, J.J., Sønderby, C.K., Sønderby, S.K., Nielsen, H., Winther, O., Hancock, J., 2017. DeepLoc: prediction of protein subcellular localization using deep learning. Bioinformatics 33 (21), 3387–3395.

Almagro Armenteros, J.J., Tsirigos, K.D., Sønderby, C.K., Petersen, T.N., Winther, O., Brunak, S., von Heijne, G., Nielsen, H., 2019. SignalP 5.0 improves signal peptide predictions using deep neural networks. Nat. Biotechnol. 37 (4), 420–423.

Bolger, A.M., Lohse, M., Usadel, B., 2014. Genome analysis Trimmomatic: a flexible trimmer for Illumina sequence data 30. Bioinformatics 30, 2114–2120.

Brethauer, S., Shahab, R.L., Studer, M.H., 2020. Impacts of biofilms on the conversion of cellulose. Appl. Microbiol. Biotechnol. 104 (12), 5201–5212.

Brown, J.L., Swift, C.L., Mondo, S.J., Seppala, S., Salamov, A., Singan, V., Henrissat, B., Drula, E., Henske, J.K., Lee, S., LaButti, K., He, G., Yan, M., Barry, K., Grigoriev, I.V., O'Malley, M.A., 2021. Co-cultivation of the anaerobic fungus Caecomyces churrovis with Methanobacterium bryantii enhances transcription of carbohydrate binding modules, dockerins, and pyruvate formate lyases on specific substrates. Biotechnol. Biofuels 14, 1–16.

Chahal, D.S., 1985. Solid-state fermentation with Trichoderma reesei for cellulase production. Appl. Environ. Microbiol. 49 (1), 205–210.

Chandrasekar, P.H., Manavathu, E.K., 2008. Do Aspergillus species produce biofilm? Future Microbiol. 3 (1), 19–21.

Dumitrache, A., Klingeman, D.M., Natzke, J., Rodriguez Jr, M., Giannone, R.J., Hettich, R.L., Davison, B.H., Brown, S.D., 2017. Specialized activities and expression differences for Clostridium thermocellum biofilm and planktonic cells. Sci. Rep. 7, 43583.

Edgar, R.C., 2010. Search and clustering orders of magnitude faster than BLAST. Bioinformatics 26, 2460–2461.

Gamarra, N.N., Villena, G.K., Gutiérrez-Correa, M., 2010. Cellulase production by Aspergillus niger in biofilm, solid-state, and submerged fermentations. Appl. Microbiol. Biotechnol. 87 (2), 545–551.

Granzier, H.L., Labeit, S., 2004. The giant protein titin: A major player in myocardial mechanics, signaling, and disease. Circ. Res. 94 (3), 284–295.

Grigoriev, I.V., Nikitin, R., Haridas, S., Kuo, A., Ohm, R., Otillar, R., Riley, R., Salamov, A., Zhao, X., Korzeniewski, F., Smirnova, T., Nordberg, H., Dubchak, I., Shabalov, I., 2014. MycoCosm portal: gearing up for 1000 fungal genomes. Nucleic Acids Res. 42 (D1), D699–D704.

Gruninger, R.J., Puniya, A.K., Callaghan, T.M., Edwards, J.E., Youssef, N., Dagar, S.S., Fliegerova, K., Griffith, G.W., Forster, R., Tsang, A., McAllister, T., Elshahed, M.S., 2014. Anaerobic fungi (phylum Neocallimastigomycota): advances in understanding their taxonomy, life cycle, ecology, role and biotechnological potential. FEMS Microbiol. Ecol. 90 (1), 1–17.

Gutiérrez-Correa, M., Ludeña, Y., Ramage, G., Villena, G.K., 2012. Recent advances on filamentous fungal biofilms for industrial uses. Appl. Biochem. Biotechnol. 167 (5), 1235–1253.

Hanafy, R.A., Lanjekar, V.B., Dhakephalkar, P.K., Callaghan, T.M., Dagar, S.S., Griffith, G.W., Elshahed, M.S., Youssef, N.H., 2020. Seven new Neocallimastigomycota genera from wild, zoo-housed, and domesticated herbivores greatly expand the taxonomic diversity of the phylum. Mycologia 112 (6), 1212–1239.

Henske, J.K., Gilmore, S.P., Haitjema, C.H., Solomon, K.V., O'malley, M.A., 2018a. Biomass-degrading enzymes are catabolite repressed in anaerobic gut fungi. AIChE J 64, 4263–4270.

Henske, J.K., Gilmore, S.P., Knop, D., Cunningham, F.J., Sexton, J.A., Smallwood, C.R., Shutthanandan, V., Evans, J.E., Theodorou, M.K., O'Malley, M.A., 2017. Transcriptomic characterization of Caecomyces churrovis: A novel, non-rhizoid-forming lignocellulolytic anaerobic fungus. Biotechnol. Biofuels 10, 305.

Henske, J.K., Wilken, S.E., Solomon, K.V., Smallwood, C.R., Shutthanandan, V., Evans, J. E., Theodorou, M.K., O'Malley, M.A., 2018b. Metabolic characterization of anaerobic fungi provides a path forward for bioprocessing of crude lignocellulose. Biotechnol. Bioeng. 115 (4), 874–884.

Hooker, C.A., Lee, K.Z., Solomon, K.V., 2019. Leveraging anaerobic fungi for biotechnology. Curr. Opin. Biotechnol. 59, 103–110.

Kim, D., Paggi, J.M., Park, C., Bennett, C., Salzberg, S.L., 2019. Graph-based genome alignment and genotyping with HISAT2 and HISAT-genotype. Nat. Biotechnol. 37 (8), 907–915.

Kovaka, S., Zimin, A.V., Pertea, G.M., Razaghi, R., Salzberg, S.L., Pertea, M., 2019. Transcriptome assembly from long-read RNA-seq alignments with StringTie2. Genome Biol. 20, 1–13.

Leggieri, P.A., Kerdman-Andrade, C., Lankiewicz, T.S., Valentine, M.T., O'Malley, M.A., 2021. Non-destructive quantification of anaerobic gut fungi and methanogens in co-culture reveals increased fungal growth rate and changes in metabolic flux relative to mono-culture. Microb. Cell Factories. 20, 1–16.

Leroy, C., Delbarre, C., Ghillebaert, F., Compere, C., Combes, D., 2008. Influence of subtilisin on the adhesion of a marine bacterium which produces mainly proteins as extracellular polymers. J. Appl. Microbiol. 105, 791–799.

Lillington, S.P., Leggieri, P.A., Heom, K.A., O'Malley, M.A., 2020. Nature's recyclers: anaerobic microbial communities drive crude biomass deconstruction. Curr. Opin. Biotechnol. 62, 38–47.

Liu, J.J., Madec, J.Y., Bousquet-Mélou, A., Haenni, M., Ferran, A.A., 2021. Destruction of Staphylococcus aureus biofilms by combining an antibiotic with subtilisin A or calcium gluconate. Sci. Reports 11, 1–12.

Love, M.I., Huber, W., Anders, S., 2014. Moderated estimation of fold change and dispersion for RNA-seq data with DESeq2. Genome Biol. 15 (550), 1–21.

Lu, S., Wang, J., Chitsaz, F., Derbyshire, M.K., Geer, R.C., Gonzales, N.R., Gwadz, M., Hurwitz, D.I., Marchler, G.H., Song, J.S., Thanki, N., Yamashita, R.A., Yang, M., Zhang, D., Zheng, C., Lanczycki, C.J., Marchler-Bauer, A., 2020. CDD/SPARCLE: The conserved domain database in 2020. Nucleic Acids Res. 48.

Marchler-Bauer, A., Bryant, S.H., 2004. CD-Search: Protein domain annotations on the fly. Nucleic Acids Res. 32.

Matsunaga, A., Tsugawa, M., Fortes, J., 2008. CloudBLAST: combining MapReduce and virtualization on distributed resources for bioinformatics applications. Proc. - 4th IEEE Int. Conf. eScience, eScience 2008 222–229.

Mitrofanova, O., Mardanova, A., Evtugyn, V., Bogomolnaya, L., Sharipova, M., 2017. Effects of Bacillus Serine Proteases on the Bacterial Biofilms. Biomed Res. Int. 2017.

Shamir, M., Bar-On, Y., Phillips, R., Milo, R., 2016. SnapShot: timescales in cell biology. Cell 164 (6), 1302–1302.e1.

Solomon, K.V., Haitjema, C.H., Henske, J.K., Gilmore, S.P., Borges-Rivera, D., Lipzen, A., Brewer, H.M., Purvine, S.O., Wright, A.T., Theodorou, M.K., Grigoriev, I.V., Regev, A., Thompson, D.A., O'Malley, M.A., 2016. Early-branching gut fungi possess a large, comprehensive array of biomass-degrading enzymes. Science 351 (6278), 1192–1195.

Swift, C.L., Brown, J.L., Seppälä, S., O'Malley, M.A., 2019. Co-cultivation of the anaerobic fungus Anaeromyces robustus with Methanobacterium bryantii enhances transcription of carbohydrate active enzymes. J. Ind. Microbiol. Biotechnol. 46 (9-10), 1427–1433.

The Gene Ontology Consortium, 2021. The Gene Ontology resource: Enriching a GOld mine. Nucleic Acids Res. 49, D325–D334.

The Gene Ontology Consortium, Ashburner, M., Ball, C.A., Blake, J.A., Botstein, D., Butler, H., Cherry, J.M., Davis, A.P., Dolinski, K., Dwight, S.S., Eppig, J.T., Harris, M. A., Hill, D.P., Issel-Tarver, L., Kasarskis, A., Lewis, S., Matese, J.C., Richardson, J.E., Ringwald, M., Rubin, G.M., Sherlock, G., 2000. Gene ontology: tool for the unification of biology. Nat, Genet, p. 25.

Theodorou, M.K., Davies, D.R., Nielsen, B.B., Lawrence, M.I.G., Trinci, A.P.J., 1995. Determination of growth of anaerobic fungi on soluble and cellulosic substrates using a pressure transducer. Microbiology 141 (3), 671–678.

Vinzelj, J., Joshi, A., Insam, H., Podmirseg, S.M., 2020. Employing anaerobic fungi in biogas production: challenges & opportunities. Bioresour, Technol, p. 300.

Wilken, S.E., Monk, J.M., Leggieri, P.A., Lawson, C.E., Lankiewicz, T.S., Seppälä, S., Daum, C.G., Jenkins, J., Lipzen, A.M., Mondo, S.J., Barry, K.W., Grigoriev, I.V., Henske, J.K., Theodorou, M.K., Palsson, B.O., Petzold, L.R., O'Malley, M.A., Lindemann, S.R., Sulheim, S., Saha, R., 2021. Experimentally Validated Reconstruction and Analysis of a Genome-Scale Metabolic Model of an Anaerobic Neocallimastigomycota Fungus. mSystems 6 (1).

Xiros, C., Studer, M.H., 2017. A Multispecies Fungal Biofilm Approach to Enhance the Celluloytlic Efficiency of Membrane Reactors for Consolidated Bioprocessing of Plant Biomass. Front. Microbiol. 8, 1930.

Yin, Y., Mao, X., Yang, J., Chen, X., Mao, F., Xu, Y., 2012. dbCAN: a web resource for automated carbohydrate-active enzyme annotation. Nucleic Acids Res. 40.

Zhao, S., Liu, Q., Wang, J.X., Liao, X.Z., Guo, H., Li, C.X., Zhang, F.F., Liao, L.S., Luo, X. M., Feng, J.X., 2019. Differential transcriptomic profiling of filamentous fungus during solid-state and submerged fermentation and identification of an essential regulatory gene PoxMBF1 that directly regulated cellulase and xylanase gene expression. Biotechnol. Biofuels 12, 103.